

PERSPECTIVES

1918 virus strains at the base of the human branch of the H1 virus evolutionary tree and some distance away from avian strains, these viruses retain avian-like receptor binding sites (5). The key receptors for influenza viruses are the sialic acids of host cell-surface glycoproteins. All avian influenza viruses replicate in the gastrointestinal tract of the host and bind to gut epithelial cells via sialic acids attached to galactose sugars in the α 2,3-linkage. In contrast, human influenza viruses replicate in the host's respiratory tract, producing distinctive disease symptoms, and bind to respiratory epithelial cells via sialic acids attached to sugars in the α 2,6-linkage. Thus, the shift from the α 2,3- to the α 2,6-linkage is crucial for enabling the switch from birds to humans and often involves signature amino acid changes in the hemagglutinin. Avian virus hemagglutinins are characterized by the amino acids glutamine-226 and glycine-228, whereas in human influenza viruses other than subtype H1, the equivalent residues are leucine-226 and serine-228. Intriguingly, human H1 viruses, including those from 1918, retain the avian amino acids at residues 226 and 228, and hence have the antigenic characteristics of avian influenza A viruses, yet are able to spread successfully through human populations.

Determination of the crystal structure of hemagglutinin from H1 viruses, including those from 1918, seems to provide a solution to the apparent paradox of how an

avian virus can spread so effectively in humans. Stevens *et al.* (3) show that despite its phylogenetic position, the hemagglutinin protein of the 1918 virus is distinctly avian in structure, particularly within the receptor binding site. The protein also has a number of important structural differences compared to other hemagglutinin subtypes, most notably at the position where the hemagglutinin is cleaved into its subunits (HA1 and HA2) and in its glycosylation pattern. Gamblin *et al.* (2) go one step further and determine the structure not only of the 1918 virus hemagglutinin but also of hemagglutinins from related H1 viruses isolated in 1930 and 1934. In the case of the 1930 and 1934 viruses, they resolved the structure of the hemagglutinin bound to its host cell receptor, enabling them to assess the binding efficiency of these proteins. Crucially, despite the avian-like residues at positions 226 and 228, H1 viruses are able to form structural conformations that bind to human cells. A combination of structural changes in the receptor-binding domain of the H1 hemagglutinin, especially changes involving the 130- and 220-loops, enables this protein to bind efficiently to the Gal-2 region of the human receptor. In sum, even though H1 viruses like those from 1918 retain the structure and antigenic characteristics of their avian ancestors, which may explain their high virulence, they have no trouble in recognizing human cells, making these viruses the perfect agents of disease.

Unveiling the crystal structure of the H1 hemagglutinin has shed new light on one of the most devastating epidemics in human history. Yet the 1918 epidemic has not given up all its secrets. A continuing enigma is whether the pandemic started as soon as the virus jumped from birds to humans, or whether there was a prepandemic period during which the virus spread in another mammalian species (perhaps the pig, which is often proposed as an intermediate host), or even in humans. If it spread in humans during this time, the devastating combination of high virulence and the ability for sustained human transmission could have been acquired (7). Perhaps the only way to answer this question is through the analysis of more archival samples, including those from the first wave of the epidemic and from avian species (8). If the virus did jump directly from birds, the children of 1918 may have been more accurate in their rhymes than anyone would have dared imagine.

References

1. J. K. Taubenberger, A. H. Reid, T. A. Janczewski, T. G. Fanning, *Philos. Trans. R. Soc. London B* **356**, 1829 (2001).
2. S. J. Gamblin *et al.*, *Science* **303**, 1838 (2004); published online 5 February 2004 (10.1126/science.1093155).
3. J. Stevens *et al.*, *Science* **303**, 1866 (2004); published online 5 February 2004 (10.1126/science.1093373).
4. A. H. Reid *et al.*, *Emerg. Infect. Dis.* **9**, 1249 (2003).
5. J. K. Taubenberger, A. H. Reid, A. E. Frafft, K. E. Bijwaard, T. G. Fanning, *Science* **275**, 1793 (1997).
6. R. G. Webster, *Proc. Natl. Acad. Sci. U.S.A.* **96**, 1164 (1999).
7. J. S. Oxford, *Philos. Trans. R. Soc. London B* **356**, 1857 (2001).
8. T. G. Fanning *et al.*, *J. Virol.* **76**, 7860 (2002).

GEOPHYSICS

Rupture in the Laboratory

Mitiyasu Ohnaka

Rupture of materials is observed over a very broad range of size scales, from atoms to macroscopic objects. Indeed, we often come across the fracture of fragile bodies such as glass in everyday life; however, among the most well-known, large-scale examples are earthquakes, which are caused when a fault in the Earth ruptures. The brittle layer where earthquakes are generated and the individual faults therein are characterized by inhomogeneity. It is therefore critically important to unravel how and where an earthquake rupture nucleates in terms of the underlying physics and seismogenic fault structure. There needs to be an understanding of

how a rupture develops spontaneously at accelerating speeds, finally reaching a steady high speed close to elastic-wave velocities. With this information, the hope is to form a comprehensive and integrated picture of the process leading up to a large earthquake in an environment conducive to seismic activity. The report by Xia *et al.* on page 1859 of this issue (1) shows how laboratory analysis can be used to understand some of the details of rupture in seismic events.

In their work, Xia *et al.* used a unique, well-designed apparatus to observe the rupture that propagates along the frictionally held interfaces of a material under uniaxial compression, which simulates a preexisting fault in Earth's crust. A high-speed camera was used to capture images of the rupture zone after the rupture was explosively triggered. The stress on the

sample was visually observed through circular polarizers and tracked during the evolution of the rupture. With this setup, they report a transition of rupture propagation at or below Rayleigh wave speeds to a much faster mode called supershear propagation. But to understand how this can occur, the basic phenomenon of rupture needs to be understood.

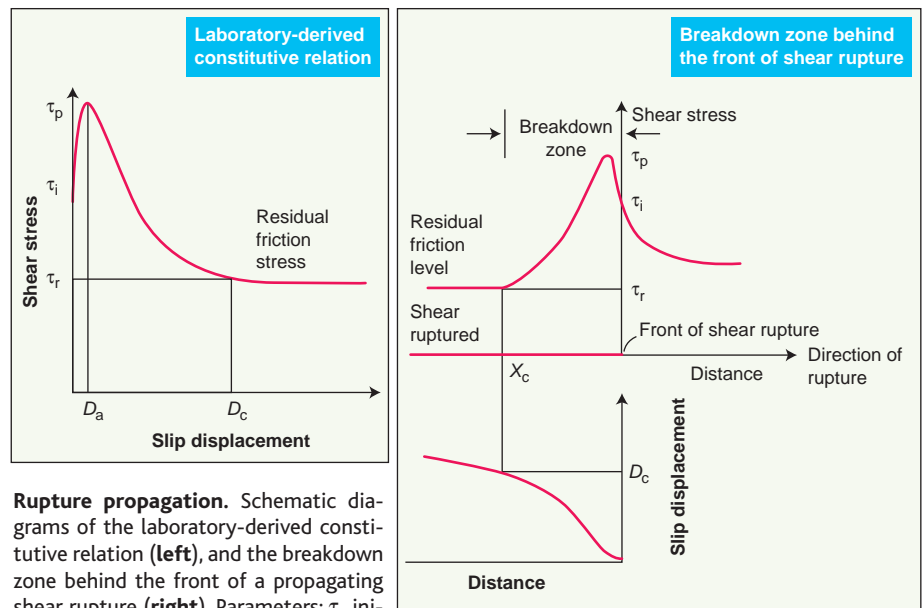
Seismological observations and their analyses (2–4) commonly show that individual faults are heterogeneous, and include areas called “asperities” or “barriers.” The presence of such asperities demonstrates that real faults comprise strong portions of high resistance to rupture growth, with the rest of the fault having low (or little) resistance to rupture growth. The resistance to rupture growth has a specific physical meaning in the framework of fracture mechanics: It is defined as the energy required for the rupture front to further grow. It has been shown that some of the asperities on an earthquake fault are strong enough to equal the strength of intact rock (5) (where shear fracture strength is the highest value of

The author is at the University of Tokyo, Bunkyo-ku, Tokyo 113, Japan, and University College London, Gower Street, London WC1E 6BT, UK. E-mail: ohnaka@g05.itscom.net

frictional strength). Such strong portions of high resistance to rupture growth are required for an adequate elastic strain energy to build up in the elastic medium surrounding the fault, as a driving force to bring about a large earthquake. It thus follows that the earthquake rupture is not a simple process of frictional slip failure, but a mixture of frictional slip failure and the fracture of initially intact rock such as an asperity fracture. Accordingly, the governing law for earthquake ruptures must be formulated as a unifying constitutive law (a relation between the shear traction and the slip displacement; see the figure, left panel) that governs both frictional slip failure and the shear fracture of intact rock.

Rupture phenomena are scale dependent; indeed, some of the physical quantities inherent in rupture exhibit scale dependence. The constitutive law must therefore be formulated so as to incorporate the scaling property; otherwise, scale-dependent physical quantities inherent in the rupture over a broad scale range cannot be treated consistently and quantitatively in terms of a single constitutive law. Real rupture surfaces of inhomogeneous rock are not flat planes, but exhibit geometric irregularity (or roughness). The shear rupture that proceeds on such irregular rupturing surfaces is governed by not only nonlinear physics of the constitutive law but also geometric properties of the rupture-surface irregularity. This is because the shear-rupture surfaces are in mutual contact and interacting during slip, which is contrasted with tensile fracture when the material is pulled apart. Laboratory experiments (5) indeed demonstrate that the fundamental cause of the scaling property lies at the characteristic length λ_c , defined as the predominant wavelength representing geometric irregularity of the rupturing surfaces. This makes it possible to formulate the constitutive law self-consistently in the framework of fracture mechanics so as to account for scale-dependent physical quantities inherent in the rupture over a broad scale range (5).

Over the past two decades, great progress has been made in understanding spontaneous earthquake-rupture propagation in terms of the underlying physics (6–9). Laboratory experiments (5, 10, 11) have demonstrated that the shear traction actually degrades transitionally with ongoing slip behind the front of a propagating shear rupture (see the figure, left panel). This laboratory-derived, slip-dependent constitutive relation is a unifying constitutive law that governs both frictional slip failure and the shear fracture of intact rock (5), and the slip-dependent law automatically satisfies the Griffith energy balance fracture criterion. Once a constitutive rela-



Rupture propagation. Schematic diagrams of the laboratory-derived constitutive relation (left), and the breakdown zone behind the front of a propagating shear rupture (right). Parameters: τ_i , initial shear stress on the verge of slip; τ_p , peak shear strength; τ_r , residual friction stress; D_a , critical slip at which the peak strength is attained; D_c , breakdown slip displacement defined as the critical slip required for the shear traction to degrade to τ_r ; and X_c , breakdown-zone length.

tion is specifically given (as shown in the figure), the stress and slip distributions at and around the rupture front can theoretically be calculated (12) (as shown in the right panel of the figure), and there is no such unrealistic stress singularity at the rupture front as predicted from linear elastic fracture mechanics. The zone behind the rupture front over which the shear traction degrades transitionally to a residual frictional stress τ_r along the fault (see the figure, right panel) is referred to as the breakdown zone. The breakdown slip displacement D_c , defined as the critical slip required for the shear traction to degrade to τ_r , is an important parameter because D_c is a constitutive parameter that scales with the characteristic length λ_c (5). It is also important because scale-dependent physical quantities inherent in the rupture can be expressed in terms of the scale-dependent constitutive parameter D_c .

For instance, the breakdown zone length X_c in the regime of dynamic shear-rupture propagation at a steady speed scales with D_c (13). The irregular rupture surfaces of a larger fault necessarily contain a longer predominant wavelength component λ_c , and accordingly D_c is larger for larger earthquakes. For typical, large earthquakes of the magnitude 8 class, for instance, D_c is estimated to be on the order of 1 m, and X_c is on the order of 1 to 10 km according to the value for $\Delta\tau_b/\tau_p$ (5), where $\Delta\tau_b$ is the breakdown stress drop defined as $\Delta\tau_b = \tau_p - \tau_r$ (τ_p , peak shear strength). It is therefore physically unreasonable to treat the rupture front as a point of stress singularity.

Thus, the conclusion by Xia *et al.* (1) that a smooth transition from sub-Rayleigh to supershear rupture propagation is plausible, and that the transition length derived from Andrews' model (6) can be modified by incorporating microcontact physics into the model is well-grounded. In the future, it is hoped that three-dimensional computer simulations will be done not only for confirming this conclusion but also for building a comprehensive and integrated model of the process leading up to a large earthquake in terms of the underlying physics in realistic, seismogenic environments.

References

1. K. Xia, A. J. Rozakis, H. Kanamori, *Science* **303**, 1859 (2004).
2. K. Aki, *J. Geophys. Res. Solid Earth* **84**, 6140 (1979).
3. H. Kanamori, G. S. Stewart, *J. Geophys. Res. Solid Earth* **83**, 3427 (1978).
4. M. Bouchon, *J. Geophys. Res. Solid Earth* **102**, 11731 (1997).
5. M. Ohnaka, *J. Geophys. Res. Solid Earth* **108** (B2), 2080, 10.1029/2000JB000123 (2003).
6. D. J. Andrews, *J. Geophys. Res. Solid Earth* **81**, 5679 (1976).
7. R. Madariaga, K. B. Olsen, in *International Handbook of Earthquake and Engineering Seismology*, Part A, W. H. K. Lee, H. Kanamori, P. C. Jennings, C. Kisslinger, Eds. (Academic Press, New York, 2002), pp. 175–194.
8. S. Das, *Pure Appl. Geophys.* **160**, 579 (2003).
9. M. Matsu'ura, P. Mora, A. Donnellan, X.-C. Yin, Eds., *Earthquake Processes: Physical Modelling, Numerical Simulation and Data Analysis*, Part I and II (Pageoph Topical Volumes, Birkhauser, Basel, 2002).
10. P. G. Okubo, J. H. Dieterich, *J. Geophys. Res. Solid Earth* **89**, 5817 (1984).
11. M. Ohnaka, Y. Kuwahara, K. Yamamoto, *Tectonophysics* **144**, 109 (1987).
12. Y. Ida, *J. Geophys. Res. Solid Earth* **77**, 3796 (1972).
13. M. Ohnaka, T. Yamashita, *J. Geophys. Res. Solid Earth* **94**, 4089 (1989).